THE JOURNAL OF PHYSICAL CHEMISTRY LETTERS
A JOURNAL OF THE AMERICAN CHEMICAL SOCIETY

pubs.acs.org/JPCL

Letter

Role of Nucleosome Sliding in the Protein Target Search for Covered DNA Sites

Anupam Mondal and Anatoly B. Kolomeisky*

Cite This: J. Phys. Chem. Lett. 2023, 14, 7073−7082

Read Online

ACCESS | Metrics & More | Article Recommendations | Supporting Information

ABSTRACT: Associations of transcription factors (TFs) with specific sites on DNA initiate major cellular processes. But DNA in eukaryotic cells is covered by nucleosomes which prevent TFs from binding. However, nucleosome structures on DNA are not static and exhibit breathing and sliding. We develop a theoretical framework to investigate the effect of nucleosome sliding on a protein target search. By analysis of a discrete-state stochastic model of nucleosome sliding, search dynamics are explicitly evaluated. It is found that for long sliding lengths the target search dynamics are faster for normal TFs that cannot enter the nucleosomal DNA. But for more realistic short sliding lengths, the so-called pioneer TFs, which can invade nucleosomal DNA, locate specific sites faster. It is also suggested that nucleosome breathing, which is a faster process, has a stronger effect on protein search dynamics than that of nucleosome sliding. Theoretical arguments to explain these observations are presented.

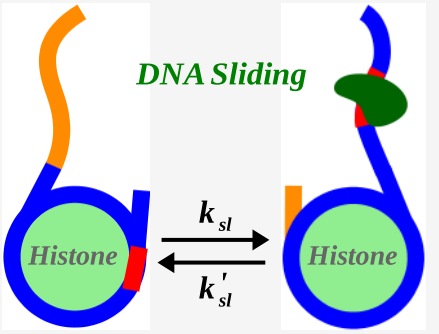

All major cellular processes associated with genetic regulation and transfer of genetic information start after protein molecules, known as transcription factors (TFs), locate specific sites on DNA, initiating a cascade of sequential biochemical processes.[1−4] In order to fit into small cellular volumes, however, in eukaryotic cells DNA molecules are bound to nucleosome structures, creating very compact chromatin structures.[5] A single nucleosome is composed of about ∼150 base pairs (bp) of DNA that are tightly wrapped into ∼1.65 superhelical left-handed turns around an octamer of histone proteins.[6,7] It is estimated that up to 90% of DNA length might be covered by nucleosomes,[1] and it seems that this might strongly reduce the accessibility of regulatory proteins, such as RNA polymerases and transcription factors, to their specific sites.[8−11] This raises an important question of how nature is capable of simultaneously fulfilling two fundamental tasks: supporting efficient genetic regulation and maintaining compact genome organization.

While crystal structures of nucleosome−DNA complexes display clear contacts between the DNA nucleotides and histone proteins,[6] the association of DNA and nucleosome is not rigid, reflecting the overall mobility of chromatin structures. Experimental studies have shown that nucleosomes are highly dynamic and the histone−DNA contacts are often disrupted spontaneously to adopt alternative conformations,[12−14] which leads to a complex multistate landscape for gene regulation. DNA wrapped around histone proteins can spontaneously unwrap and rewrap at nucleosome termini in a process termed nucleosome breathing.[15−21] The momentary exposure of nucleosomal DNA due to thermal fluctuations provides an opportunity for regulatory proteins to efficiently access the otherwise nucleosome-covered DNA sites.[17,18,22−24] A recent study based on the cryo-EM experiment has successfully characterized distinct conformations of partially unwrapped structures with varying lengths of liberated DNA segments,[14] and it underscored the functional importance of breathing dynamics for the invasion of DNA-binding proteins to nucleosomal DNA. Indeed, nucleosome breathing has been found to play a pivotal role in transcriptional elongation,[25,26] and it was also argued that it might promote liquid−liquid phase separation by maintaining the structural plasticity of the nucleosomes inside the cell nucleus.[27]

Although it is now well established that nucleosome breathing is crucial for regulating various genetic processes, there is another mode of nucleosome mobility, sliding, that has received relatively less attention.[13,28−32] In this process, the center of mass of the whole nucleosome complex moves along the DNA chain by simultaneously breaking and creating multiple DNA−histone contacts. Such highly coordinated motion contrasts with nucleosome breathing in which only unwrapping (breaking of the bonds) or only wrapping (creating of the bonds) is taking place. The effective free-energy landscape for nucleosome sliding is also different from that for nucleosome breathing. While the profile for breathing has a nonzero slope with the fully wrapped state being thermodynamically more stable (lower in free energy) than the

Received: June 21, 2023
Accepted: July 28, 2023
Published: August 1, 2023

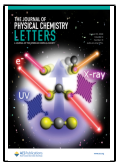

https://doi.org/10.1021/acs.jpclett.3c01704
J. Phys. Chem. Lett. 2023, 14, 7073−7082

unwrapped state, the profile for sliding has a zero slope because the states before and after sliding have approximately the same free energy.

Experimental studies indicate that the sliding rates depend on the DNA sequence and length of the DNA fragment between the neighboring nucleosomes.[33−35] It has been also suggested that the inherent mobility of nucleosomes can be altered by the deletion of histone tails[36] and/or mutations in histone proteins.[37] Recent high-speed atomic force microscopy investigations[13,38] have successfully captured spontaneous reversible sliding of mononucleosomes on a subsecond time scale with high temporal resolution. Another single-molecule study[39] probed the diffusion of nucleosomes with a base-pair scale resolution on natural, biologically relevant sequences. These measurements yielded the estimate for the diffusion constant of the nucleosome on DNA, $D \simeq 1.3 \pm 0.14$ bp^2 s^{-1}. It is important to note that this diffusion constant reflects multiple runs and pauses during nucleosome sliding. This means that the nuclesome can slide relatively fast but then it will pause for a significant amount of time before the next move.

Recent theoretical investigation[40] has attempted to evaluate the effect of nucleosome sliding in a protein target search for specific sites by analyzing a coarse-grained stochastic model in which the DNA sites that are facing outward from the histone protein are assumed to be accessible and those sites that are in close proximity to the histone proteins remain inaccessible. Using analytical calculations and computer simulations, a description of the protein target search process was obtained, clarifying some important differences between nucleosome breathing and nucleosome sliding. However, there are some issues with this theoretical approach. The quantitative estimates of the search times are too large (several hours) compared to experimental estimates (several minutes). Clearly, such long search times will not activate genes fast enough for the proper functioning of living cells.[41] In addition, a fixed sliding length of 5 bp is assumed in these calculations while experimental measurements suggest that a nucleosome can slide 40−50 bp at each event.[13]

To understand the molecular mechanisms of the protein target search for nucleosome-covered DNA sites, it is essential to notice that all TFs can be divided into two large classes depending on their ability to invade nucleosomes. Those proteins that are capable of finding their specific sites despite the presence of nucleosomes are known as pioneer TFs.[42−46] Those proteins that are not able to penetrate nucleosomes are known as normal or nonpioneer TFs. Pioneer TFs are first in opening chromatic structures, allowing normal TFs then to locate their specific sites on DNA.[43,47,48] Recent experiments suggest that pioneer TFs might trigger diverse transcriptional programs, and their binding can lead to opening silent chromatin regions.[48−51] The ability of pioneer TF binding to target motifs on DNA embedded in nucleosomes therefore has a profound effect on the expression levels of genes. Several theoretical studies have been already proposed to explain how pioneer TFs find their nucleosomal targets, showing that pioneer TFs are more efficient in locating specific sites than any other nonpioneer TFs.[22,52] In addition, an idea of an interaction−compensation mechanism to explain the ability of pioneer TFs to enter the nucleosome has been proposed.[24] According to this idea, pioneer TFs invade nucleosomes by substituting DNA−nucleosome bonds with similar DNA−TF bonds, effectively displacing the nucleosome from DNA. It was also argued that pioneer TFs might take advantage of nucleosome breathing dynamics in their search for hidden DNA sites.[24] However, still unclear are how nucleosome sliding affects the dynamics of the protein target search for DNA sites covered by nucleosomes and the differences between nucleosome breathing and nucleosome sliding for these processes.

In this Letter, we present a theoretical investigation of the role of nucleosome sliding in the protein target search for nucleosome-covered DNA sites and how it compares with the effect of nucleosome breathing. A discrete state stochastic model based on the interaction-compensation mechanism, according to which the pioneering TFs displace the histone−DNA interactions and replace them with similar protein−DNA interactions, is introduced. By solving explicitly this model using the method of first-passage probabilities and supplementing analytical calculations with Monte Carlo computer simulations, a comprehensive description of protein target search dynamics is obtained. Our results indicate that the sliding length is an important parameter that controls the details of the search mechanisms. While for longer lengths nonpioneer TFs seem to be more efficient in locating their targets for most DNA sites, for shorter (and more realistic) sliding lengths pioneer TFs perform much better. Increasing the sliding rate makes pioneer TFs even more efficient. In addition, theoretical calculations show that, for experimentally measured kinetic rates, the impact of nucleosome breathing on the target search is stronger than for the nucleosome sliding. Physical-chemical arguments to explain these observations are presented. It is important to emphasize that our theoretical analysis is driven by experimental observations, and in all calculations, we utilized experimentally measured parameters as much as possible.

Let us consider a system consisting of a linker DNA segment attached to another DNA segment with bound nucleosome particles, as illustrated in Figure 1A. The nucleosomal DNA (blue-colored segment) is fully wrapped around the histone core octamer (green circle) that covers Δ sites, and the linker DNA length is l (orange-colored segment). The total DNA length is then equal to the $L = l + \Delta$ sites. We model the DNA molecule as a lattice of L sites, where each site is equivalent to about 10 bps, which is the typical size of the specific region on DNA to which the TFs are binding (the size of the target).[4,53] It is assumed that the sliding of the nucleosome can take place only between two conformations (Figure 1A). In one conformation, the nucleosome is positioned to the right side of the linker DNA (nucleosome right, NR) while in another conformation, the nucleosome rolls over the linker DNA and the same length l of DNA becomes free. This corresponds to the position of the nucleosome on the left side of the free DNA segment (nucleosome left, NL). Note that the size of the nucleosome Δ (i.e., the number of sites) remains the same in both conformations. In our theoretical description, we define the linker length l as the sliding length; i.e., the nucleosome reversibly moves over the distance of l sites. The transition rate from NR to NL is equal to k_{sl}, while the reverse transition rate is k'_{sl}. Since both conformations (NR and NL) are assumed to have the same free energy, we take $k_{sl} = k'_{sl}$. These rates can be estimated from the knowledge of the diffusion coefficient for sliding nucleosomes[39]

$$t = \frac{l^2}{2D} \tag{1}$$

https://doi.org/10.1021/acs.jpclett.3c01704
J. Phys. Chem. Lett. 2023, 14, 7073−7082

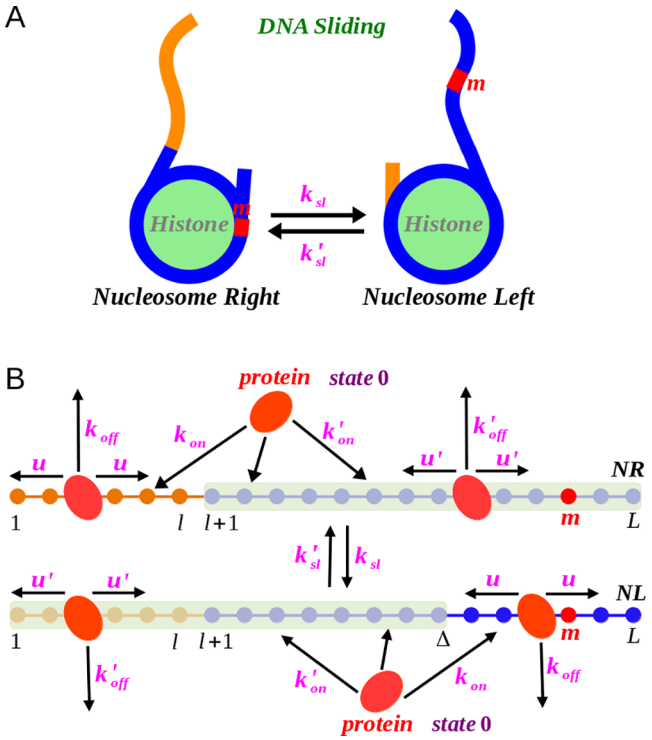

Figure 1. (A) Schematic representation of the nucleosome sliding between two conformations. The histone particle can be located at the right end of the DNA segment (Nucleosome Right) or at the left end of the DNA segment (Nucleosome Left). The transition rates between the two conformations are equal to $k_{sl} = k'_{sl}$. The red patch located at site m denotes the target site. (B) Schematic representation of the discrete-state stochastic model for protein target search with the nucleosome sliding. Black arrows correspond to all possible transitions in the system as explained in the text. The search is accomplished when the protein molecule (red ellipse) reaches its target site (red circle) located at site m.

For example, if the sliding length is equal to $l = 5$ (50 bp) we obtain $k_{sl} = 1.04 \times 10^{-3}$ s^{-1}, and for $l = 10$ (100 bp) we obtain $k_{sl} = 2.6 \times 10^{-4}$ s^{-1}. One can notice that realistic sliding rates seem to be quite slow in comparison with other dynamic processes in the system.

To explicitly analyze the protein target search process on DNA in the system with nucleosome sliding, we consider a discrete-state stochastic model, as presented in Figure 1B. It is assumed that at time $t = 0$ the protein molecule starts the search process from the bulk solution, and this is labeled as state 0. From the solution, the protein can associate to any DNA site, but the association rates depend on whether the DNA segment is nucleosome-covered or naked. The association rate with the free DNA sites is equal to k_{on} (per unit site), while the corresponding association rate with the nucleosome-covered DNA sites is k'_{on} (see Figure 1B). Similarly, the dissociation rates from the free and nucleosome-covered DNA sites into the solution are given by k_{off} and k'_{off}, respectively. In addition, the nonspecifically bound protein can slide along the nucleosome-free region with rate u, while the sliding rate along the nucleosome-covered DNA segment is equal to u' (Figure 1B). The system also fluctuates between two conformational states, NR and NL, with transition rates of $k_{sl} = k'_{sl}$. The search process continues until the protein reaches the target sequence located at site m ($1 \le m \le L$) for the first time in any of the nucleosome conformations.

Most of the transition rates described above have been measured experimentally,[54−56] and in our theoretical calculations we will utilize them. More specifically, it was found that the binding rates are similar for both pioneer and nonpioneer TFs; however, the dissociation rates of pioneer TFs are much slower from the nucleosome-covered region compared to nonpioneer TFs, and the situation is completely reversed for the dissociations from the free DNA segments. To explain these observations, we recently proposed an idea of an interaction-compensation mechanism in which it was suggested that the pioneer TFs might weaken some bonds between the histone protein and DNA and replace them with similar TF−DNA interactions.[24,45,52] The structural similarity between pioneer TFs and linker histone proteins from the nucleosome stimulated this proposal. It was also supported by a recent experimental study that combined single-molecule fluorescence, cryo-EM, and live-cell measurements, indicating that a basic helix−loop−helix of a budding yeast pioneer TF enables efficient nucleosome invasion.[57] Such interactions, therefore, allow pioneer TFs not only to successfully invade nucleosome-covered DNA but also to increase their residence times on nucleosomes. It is also assumed that the interaction−compensation mechanism might enable the pioneer TFs to slide faster along the nucleosome-covered DNA segments as compared to any nonpioneer TF, while the completely opposite behavior is expected on free DNA segments.[24,52] This leads to different transition rates on free and nucleosome-covered DNA sites for both pioneer and nonpioneer TFs, as shown in Table 1.

Table 1. Transition Rates for Pioneer and Normal TFs[a]

TF	u (s^{-1})	u' (s^{-1})	k_{on} (s^{-1})	k'_{on} (s^{-1})	k_{off} (s^{-1})	k'_{off} (s^{-1})
nonpioneer	10	1	10^{-2}	10^{-4}	10^{-2}	1
pioneer	1	10	10^{-2}	10^{-4}	1	10^{-2}

[a]The data are adopted from a combination of ensemble, single-molecule, and live-cell fluorescence experiments.[54−56]

To obtain a comprehensive dynamic description of the protein search process in the system with nucleosome sliding, we utilize a method of first-passage probabilities that have been successfully explored before for investigating various dynamic aspects of protein−DNA interactions.[4,22,24,58,59] In this approach, probability density functions $F_n^{NR}(t)$ and $F_n^{NL}(t)$ for DNA sites $n = 1, ..., L$ are introduced. They are defined as the first-passage probability for the protein to reach the target site located at position m at time t for the first time if at $t = 0$ the protein started at site n on DNA in the NR or NL conformation. One can also define first-passage probability functions $F_0^{NR}(t)$ and $F_0^{NL}(t)$ to reach the target site at time t, if at $t = 0$ the protein was in the bulk solution (state 0) and the nucleosome is in the NR (or NL) conformational state. Then the temporal evolution of these probabilities can be described by a set of backward master equations,[24,52]

$$\frac{dF_n^{NR}(t)}{dt} = u[F_{n-1}^{NR}(t) + F_{n+1}^{NR}(t)] + k_{off}F_0^{NR}(t) + k_{sl}F_n^{NL}(t) - (2u + k_{off} + k_{sl})F_n^{NR}(t) \quad (2)$$

for the linker DNA segment with $1 < n \le l$ in NR conformation and

https://doi.org/10.1021/acs.jpclett.3c01704
J. Phys. Chem. Lett. 2023, 14, 7073−7082

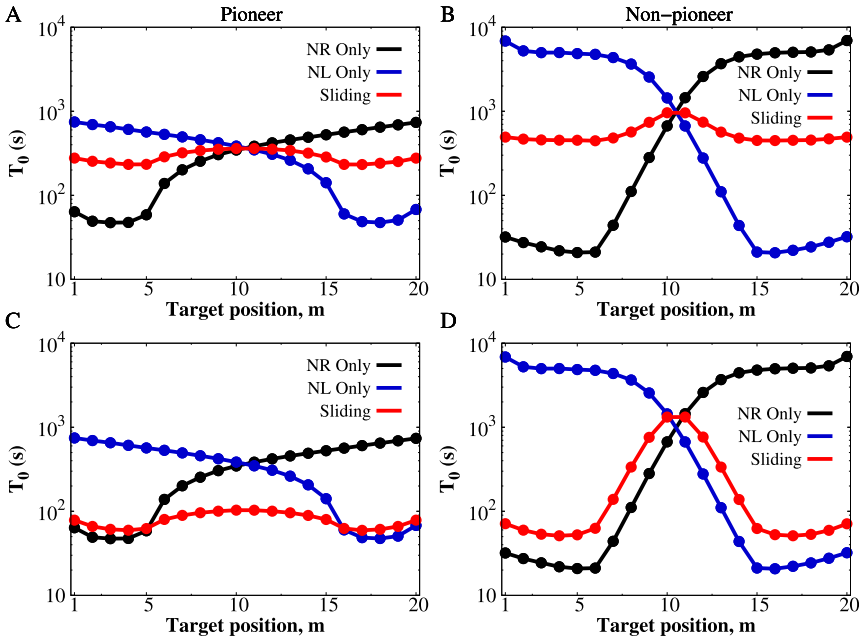

Figure 2. Mean search times as a function of the target position on DNA for pioneer TFs in (A) and (C) and nonpioneer TFs in (B) and (D). Three different situations are considered: when the nucleosome is always positioned at the right end of the DNA chain (NR, black curves) and always at the left end (NL, blue curves) and when the nucleosome is sliding (red curves). Analytical results are presented by solid lines, and symbols are from Monte Carlo simulations. The error bars for each symbol are defined as the standard errors, and the associated error bars are smaller than the symbol size. The following parameters are used in calculations: $l = 5$, $\Delta = 15$, $L = l + \Delta$, and all other transition rates are as given in Table 1. For (A) and (B) we also used $k_{sl} = k'_{sl} = 1.04 \times 10^{-3}$ s^{-1}, while for (C) and (D) we used $k_{sl} = k'_{sl} = 1$ s^{-1}.

$$\frac{dF_n^{NR}(t)}{dt} = u'[F_{n-1}^{NR}(t) + F_{n+1}^{NR}(t)] + k'_{off}F_0^{NR}(t) + k_{sl}F_n^{NL}(t) - (2u' + k'_{off} + k_{sl})F_n^{NR}(t) \quad (3)$$

for the nucleosome-covered DNA region with $l + 1 \le n < L$ in NR conformation. Similarly,

$$\frac{dF_n^{NL}(t)}{dt} = u'[F_{n-1}^{NL}(t) + F_{n+1}^{NL}(t)] + k'_{off}F_0^{NL}(t) + k'_{sl}F_n^{NR}(t) - (2u' + k'_{off} + k'_{sl})F_n^{NL}(t) \quad (4)$$

for the nucleosome-covered DNA region with $1 < n \le \Delta$ in NL conformation; and

$$\frac{dF_n^{NL}(t)}{dt} = u[F_{n-1}^{NL}(t) + F_{n+1}^{NL}(t)] + k_{off}F_0^{NL}(t) + k'_{sl}F_n^{NR}(t) - (2u + k_{off} + k'_{sl})F_n^{NL}(t) \quad (5)$$

for the nucleosome-free DNA region with $\Delta + 1 \le n < L$ in the NL conformation.

The dynamics at the boundaries ($n = 1$ and $n = L$) are slightly different, leading to

$$\frac{dF_1^{NR}(t)}{dt} = uF_2^{NR}(t) + k_{off}F_0^{NR}(t) + k_{sl}F_1^{NL}(t) - (u + k_{off} + k_{sl})F_1^{NR}(t) \quad (6)$$

$$\frac{dF_L^{NR}(t)}{dt} = u'F_{L-1}^{NR}(t) + k'_{off}F_0^{NR}(t) + k_{sl}F_L^{NL}(t) - (u' + k'_{off} + k_{sl})F_L^{NR}(t) \quad (7)$$

$$\frac{dF_1^{NL}(t)}{dt} = u'F_2^{NL}(t) + k'_{off}F_0^{NL}(t) + k'_{sl}F_1^{NR}(t) - (u' + k'_{off} + k'_{sl})F_1^{NL}(t) \quad (8)$$

$$\frac{dF_L^{NL}(t)}{dt} = uF_{L-1}^{NL}(t) + k_{off}F_0^{NL}(t) + k'_{sl}F_L^{NR}(t) - (u + k_{off} + k'_{sl})F_L^{NL}(t) \quad (9)$$

In addition, if the process starts in the bulk solution ($n = 0$), we have

$$\frac{dF_0^{NR}(t)}{dt} = k_{sl}F_0^{NL}(t) + k_{on}\sum_{n=1}^{l}F_n^{NR}(t) + k'_{on}\sum_{n=l+1}^{L}F_n^{NR}(t) - [k_{sl} + lk_{on} + (L - l)k'_{on}]F_0^{NR}(t) \quad (10)$$

$$\frac{dF_0^{NL}(t)}{dt} = k'_{sl}F_0^{NR}(t) + k'_{on}\sum_{n=1}^{\Delta}F_n^{NL}(t) + k_{on}\sum_{n=\Delta+1}^{L}F_n^{NL}(t) - [k'_{sl} + \Delta k'_{on} + (L - \Delta)k_{on}]F_0^{NL}(t) \quad (11)$$

Furthermore, the initial condition is $F_m^{NR}(t) = \delta(t)$ or $F_m^{NL}(t) = \delta(t)$, which means that if the searching protein is already at the target site m at $t = 0$ in any of two nucleosome conformations, the search process ends immediately.

Transforming eqs 2−11 using Laplace transformations [$\widetilde{F_n^{NR}}(s) \equiv \int_0^\infty e^{-st}F_n^{NR}(t)\,dt$ and $\widetilde{F_n^{NL}}(s) \equiv \int_0^\infty e^{-st}F_n^{NL}(t)\,dt$], they can be exactly solved for all ranges of parameters. Detailed calculations are presented in the Supporting Information. To quantify the target search dynamics, we evaluate mean target search times,

https://doi.org/10.1021/acs.jpclett.3c01704
J. Phys. Chem. Lett. 2023, 14, 7073−7082

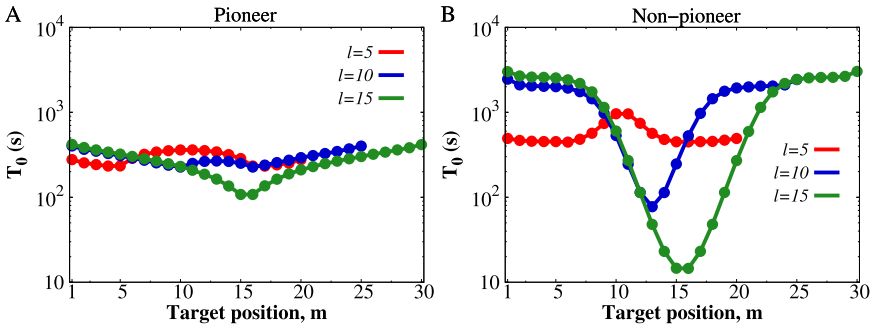

Figure 3. Mean search times as a function of the target position for three different sliding lengths for (A) pioneer and (B) nonpioneer TFs. Analytical results are presented by solid lines, and symbols are from Monte Carlo simulations. The following parameters are used in calculations: $\Delta = 15$, $L = l + \Delta$, $k_{sl} = k'_{sl}$ are determined from eq 1, and all other transition rates are given in Table 1.

$$T_0^{NR} \equiv \int_0^\infty t F_0^{NR}(t)\, dt = -\left.\frac{\partial \widetilde{F_n^{NR}}(s)}{\partial s}\right|_{s=0} \tag{12}$$

and

$$T_0^{NL} \equiv \int_0^\infty t F_0^{NL}(t) dt = -\left.\frac{\partial \widetilde{F_n^{NL}}(s)}{\partial s}\right|_{s=0} \tag{13}$$

Since the target search process can start with an equal probability for the nucleosome to be found in any of two conformational states, it is important to average out the mean search times,

$$T_0 = \frac{k_{sl}}{k_{sl}+k'_{sl}} T_0^{NL} + \frac{k'_{sl}}{k_{sl}+k'_{sl}} T_0^{NR} = \frac{1}{2} T_0^{NL} + \frac{1}{2} T_0^{NR} \tag{14}$$

To make our theoretical analysis relevant for understanding cellular processes, in our calculations, we utilized as many realistic parameters as possible. As discussed above, most of the transitions used in our calculations (as presented in Table 1) come from experimental measurements. In addition, to mimic real nucleosomes, we chose the size of the fully wrapped nucleosome as $\Delta = 15$ because each site in our model (Figure 1B) corresponds to 10 bp, and ∼150 bp of DNA is wrapped around the histone octamer. Furthermore, the average length of the linker DNA between neighboring nucleosomes, often known as nucleosome repeat length (NRL), varies widely between organisms and even between different cell types of the same organism, ranging from ∼50 bp to ∼200 bp.[30,31,60,61] Therefore, in our calculations, mean search times are evaluated for different linker lengths, namely, $l = 5$, $l = 10$, and $l = 15$.

To quantify the effect of sliding, theoretical calculations for the system with sliding are compared with the situations without sliding when the nucleosome is always frozen in the conformation NL or in the conformation NR. The results are presented in Figure 2 for both pioneer and nonpioneer TFs. As one can see, in the frozen configurations (black and blue curves), it is faster to locate target sites on free DNA segments, but pioneer TFs perform better for covered sites and nonpioneer TFs search faster on the free DNA segments.[52] Turning on nucleosome sliding (red curves in Figure 2) modifies target search dynamics. It is now faster to find the sites that were covered before in frozen configurations, while it is slower to find sites that were free in frozen configurations. This average behavior (Figure 2A,B) is expected because the system fluctuates between two limiting conformations NR and NL, freeing different parts of DNA in alternating fashion. But it is important to note that under the same conditions the pioneer TFs find their targets faster than the nonpioneer TFs. Increasing the sliding rate (Figure 2C,D) as suggested by high-speed AFM experiments[13] makes the pioneer TFs even more efficient in locating target sites. Our calculations suggest that the pioneer TFs locate targets faster than the nonpioneer TFs (depending on the sliding rate), and the estimated search times (with $k_{sl} = 1.04 \times 10^{-3}$ s^{-1}) for the hidden DNA sites (∼280−360 s) are consistent with recent experimental measurements of search times for pioneer TF GAF in *in vivo* conditions.[41]

It is essential to emphasize here that we consider the sliding length of $l = 5$ (or 50 bp) in a single sliding event for our calculations. One may argue here that for a single sliding event, disrupting all bonds and then simultaneously breaking and reforming all histone−DNA contacts in a bulk sliding would presumably lead to a very high free-energy penalty. Experimental studies suggest that nucleosome sliding can occur through two mechanisms: twist diffusion or loop/bulge propagation.[29,62,63] In the twist diffusion model, a twist defect is generated in a segment of nucleosomal DNA and then it diffuses around the nucleosome in a corkscrew-like motion, whereas in the loop/bulge propagation model, DNA loops or bulges are formed on one side of the nucleosome and then propagate around the histone core to emerge on the other side in an inchworm-like motion. In both cases, nucleosome diffusion is a stepwise motion: ∼1 bp for twist diffusion and ∼10 bp for loop propagation at a time, respectively. In order to mimick the effect of such diffusive motion of nucleosomes, we also investigated a stepwise sliding between the NR and NL conformations (see Supplementary Figure S1) with a step size of 10 bp (or 1 DNA site). The corresponding results are obtained from Monte Carlo simulations and presented in Supplementary Figure S2. One can see that the main conclusions of the theoretical analysis remain the same for both stepwise and two-state sliding models, suggesting that our simplest model is good enough to describe the actual events during nucleosome sliding.

Experimental studies suggest that the length of DNA linkers between neighboring nucleosomes (NRL) is an important factor that can influence protein−DNA interactions.[64] In our theoretical approach, the role of DNA linkers can be directly tested by varying the length of free DNA segments l. The results of the corresponding calculations are shown in Figure 3, where the mean search times for pioneer and nonpioneer TFs are evaluated for three different sliding lengths $l = 5$, $l = 10$, and $l = 15$. Significant differences in target search dynamics are

https://doi.org/10.1021/acs.jpclett.3c01704
J. Phys. Chem. Lett. 2023, 14, 7073−7082

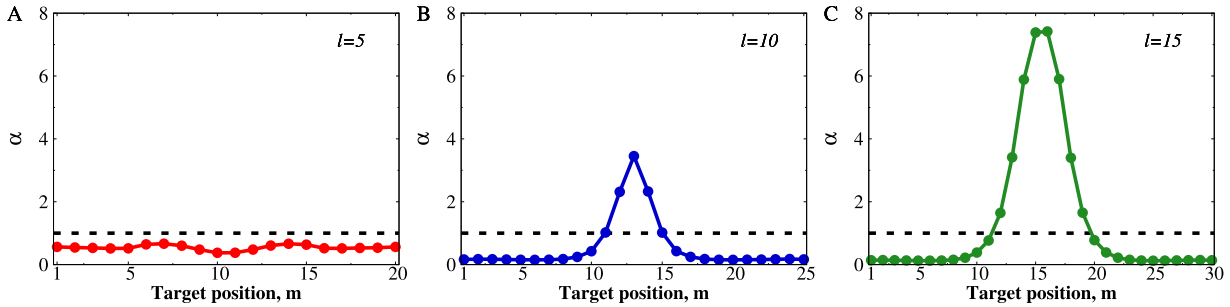

Figure 4. Acceleration in the mean search times for the system with nucleosome sliding for pioneer TFs in comparison with nonpioneer TFs as a function of the target position for (A) $l = 5$, (B) $l = 10$, and (C) $l = 15$. Analytical results are presented by solid lines, and symbols are from Monte Carlo simulations. The following parameters are used in calculations: $\Delta = 15$, $L = l + \Delta$, and $k_{sl} = k'_{sl}$ are calculated from eq 1 depending on the sliding length l, and all other transition rates are given in Table 1. Dashed horizontal lines correspond to $\alpha = 1$.

found for the two types of TFs. While for pioneer TFs increasing the sliding length has a relatively weak effect (Figure 3A), much stronger changes are observed for nonpioneer TFs (Figure 3B). To quantify this effect, we introduce a dimensionless acceleration parameter,

$$\alpha(m, l) = \frac{T_{0,\text{pioneer}}(m, l)}{T_{0,\text{non-pioneer}}(m, l)} \tag{15}$$

It specifies how much faster it is to find the target located at the site m for nonpioneer TFs in comparison with pioneer TFs for given sliding length l. Thus, $\alpha < 1$ corresponds to pioneer TFs being faster, while for $\alpha > 1$ nonpioneer TFs locate their targets faster.

The comparison of target search dynamics for different sliding lengths is presented in Figure 4 where the acceleration parameter α is evaluated for different values of l. One can see that, for short sliding length ($l = 5$), pioneer TFs are always faster, and the location of the target does not play any role (Figure 4A). The situation changes for longer sliding lengths ($l = 10$ and $l = 15$). Pioneer TFs are still faster for target sites located closer to the ends of the system, but for the sites in the middle, nonpioneer TFs are becoming faster: see Figure 4B,C. Those are the sites that although occasionally covered by nucleosomes during the sliding fluctuations are closest to the border with the free DNA segment. The accelerations of up to $\alpha \simeq 4$ ($l = 10$) and $\alpha \simeq 8$ ($l = 15$) are observed.

To emphasize the difference in the target search dynamics as a function of the sliding length, in Figure 5 we present the

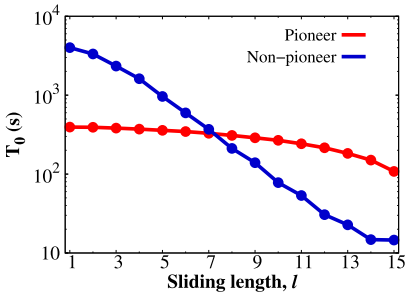

Figure 5. Mean search times as a function of the sliding length l for pioneer and nonpioneer TFs. At each value of l, the position of the target site $m = L/2$ is chosen. Analytical results are presented by solid lines, and symbols are from Monte Carlo simulations. The following parameters are used in calculations: $\Delta = 15$, $L = l + \Delta$, $k_{sl} = k'_{sl}$ are calculated from eq 1, and all other transition rates are given in Table 1.

mean search times for pioneer TFs (red curve) and nonpioneer TFs (blue curve) for the target located at $m = L/2 = (l + \Delta)/2$. One can see that pioneer TFs are faster for relatively short sliding lengths ($l \leq 7$), and generally mean search times T_0 slowly decrease as a function of l. For longer sliding lengths ($l > 7$), the nonpioneer TFs are becoming faster. In addition, the mean search times exhibit a much stronger decrease as a function of l. Importantly, a similar trend is also observed if one considers a more realistic situation where linker DNA (of similar length) is attached on both sides of the nucleosome (see Supplementary Figures S3 and S4) and the nucleosome core slides on either side of the linker DNA stochastically.

Our theoretical approach allows us to present possible microscopic arguments to explain these observations. The transition rates (see Table 1) indicate that both the pioneer and nonpioneer TFs prefer to associate to the DNA linker region by coming directly from the solution ($k_{on} \simeq 10^{-2}$ s^{-1}) rather than to bind to the nucleosome-covered region ($k'_{on} \simeq 10^{-4}$ s^{-1}). Then both types of transcription factors mostly enter the nucleosome-covered segment by sliding from the linker DNA region.[24] For the pioneer TFs, the dissociation rate from the linker DNA segment is fast ($k_{off} \simeq 1$ s^{-1}), while from the nucleosome-covered region, it dissociates rather slowly ($k'_{off} \simeq 10^{-2}$ s^{-1}). On the contrary, the nonpioneer TFs prefer the linker DNA region ($k_{off} \simeq 10^{-2}$ s^{-1}) and they dissociate much faster from the nucleosome-covered region ($k'_{off} \simeq 1$ s^{-1}). In addition, the pioneer TFs slide relatively faster ($u' \simeq 10$ s^{-1}) along the nucleosome-covered DNA segment than along the DNA linker region ($u \simeq 1$ s^{-1}), while the nonpioneer TFs exhibit the opposite trend ($u > u'$). As a result, when the sliding length l is relatively short, the pioneer TFs might quickly enter the nucleosome-covered region from the DNA linker region, and they can stay there long enough to find their targets. This is because the free DNA segment is so short that the pioneer TFs on average land on the DNA linker not far away from the border with the covered region ($\sim l/2$ distance from the start of the nucleosome-covered region), and so they can slide before being dissociated into the solution. When the sliding length is relatively large, the pioneer TFs have a higher chance to dissociate from the linker DNA region before entering the nucleosome-covered region because, on average, they land farther away from the border. However, the situation is different for nonpioneer TFs. The longer the length of the free DNA segment, the longer nonpioneer TFs can stay on the DNA linker region (slow dissociation) and reach the nucleosome (fast sliding), allowing them to find the targets faster for sites that are not far away from the border. But the

https://doi.org/10.1021/acs.jpclett.3c01704
J. Phys. Chem. Lett. 2023, 14, 7073−7082

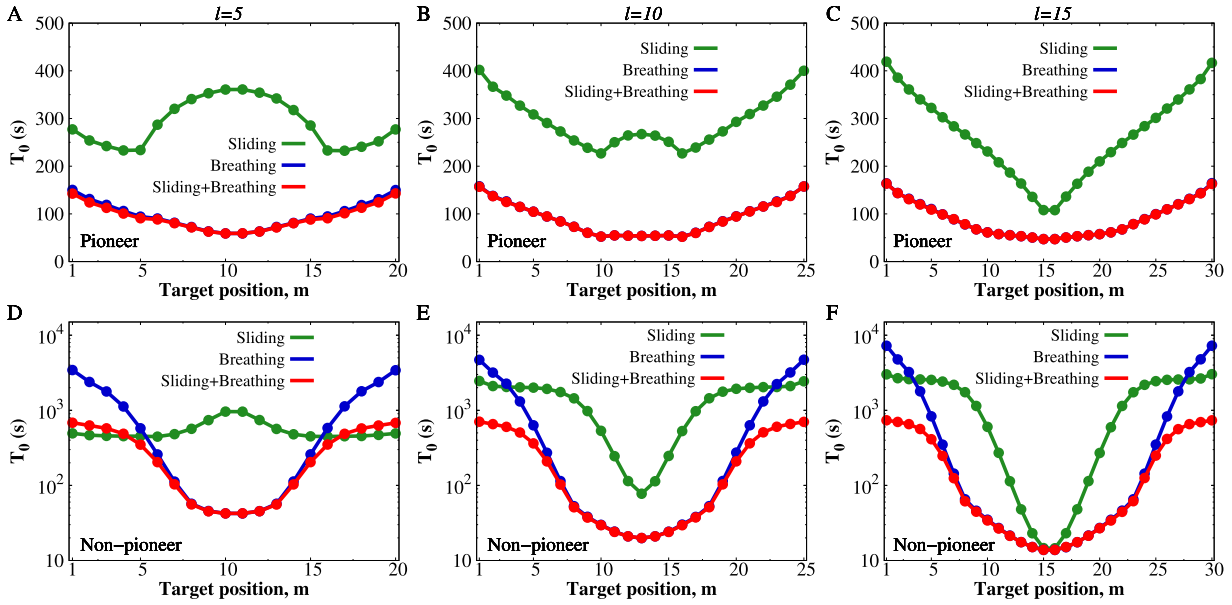

Figure 6. Mean search times as a function of the target position for pioneer TF for (A) $l = 5$, (B) $l = 10$, and (C) $l = 15$. Three different situations are considered: when the nucleosome is sliding (green curves), when the nucleosome is breathing (blue curves), and when the nucleosome is performing both sliding and breathing dynamics (red curves). (D−F) Similar analysis is performed for nonpioneer TFs. Analytical results are presented by solid lines, and symbols are from Monte Carlo simulations. The following parameters are used in calculations: $\Delta = 15$, $L = l + \Delta$, $l_B = 7$, $k_{open} = 210\ s^{-1}$, $k_{close} = 370\ s^{-1}$, $k_{sl} = k'_{sl}$ are determined from eq 1 depending on the sliding length l, and all other transition rates are those as described in Table 1.

nonpioneer TFs cannot locate sites that are too far from the border between the segments because they quickly dissociate from the nucleosome-covered region (fast dissociation). At the same time, the pioneer TFs, although they have difficulties reaching the nucleosome region, stay there longer (low dissociation), and for this reason they are more successful in locating sites that are farther away from the border between segments. It is also important to notice that due to nucleosome sliding the border between covered and free DNA segments fluctuates between the locations at l and $L - l$.

It is important to discuss the relevance of these results for biological systems. Experiments suggest that sliding lengths most probably are not too long,[13] suggesting that in real systems pioneer TFs can significantly accelerate the protein target search. It is also possible that the kinetic rates of these proteins are tuned by evolution to achieve the fastest opening rates of chromatin structures that exhibit nucleosome sliding.

Theoretical calculations show that nucleosome sliding strongly influences the protein target search. But our analysis does not take into account another important mode of mobility, nucleosome breathing. At the same time, we recently developed a discrete stochastic model to analyze the role of nucleosome breathing in the protein target search.[24] In this model, the system fluctuates between fully wrapped and partially unwrapped conformations, and it can be easily extended to our system, which also has the DNA linker segment (see Supplementary Figure S5). The details of such calculations are presented in the Supporting Information. Now we can combine nucleosome breathing and nucleosome sliding and investigate how all aspects of nucleosome mobility influence the dynamics of finding special sites on nucleosome-covered DNA.

The results of our calculations that compare the effects of nucleosome breathing and nucleosome sliding on the protein target search are shown in Figure 6. As one can see (Figure 6A−C), for pioneer TFs nucleosome breathing dominates for all ranges of parameters, and the role of nucleosome sliding is really negligible. The situation is only slightly different for nonpioneer TFs (Figures 6D−F). Nucleosome breathing dominates the target search for DNA sites that are in the middle of the system, while for sites at the DNA ends, both breathing and sliding are equally important. Increasing the sliding length makes the contribution of breathing more important. To explain these observations, we notice that nucleosome sliding is a relatively slow process: $k_{sl} \simeq 1.04 \times 10^{-3}\ s^{-1}$ for $l = 5$. At the same time, nucleosome breathing is much faster: in our calculations, we utilized $k_{open} = 210\ s^{-1}$ and $k_{close} = 370\ s^{-1}$ as estimated in recent single-molecule experiments.[16] It is important to note that our theoretical predictions for mean search times agree well with the recent *in vivo* kinetic measurements for GAGA pioneer TF.[41]

To summarize, we developed a theoretical method to investigate the role of nucleosome sliding in the protein target search for specific sites on DNA. It is based on the discrete-state stochastic description of the most relevant physical-chemical processes that allowed us to explicitly obtain dynamic properties of the system by using a method of first-passage probabilities. Analytical calculations are further supplemented by Monte Carlo computer simulations. The theoretical method is applied to analyzing the target search dynamics for both pioneer and nonpioneer TFs using experimentally measured parameters for these proteins. It is found that nucleosome sliding allows proteins to find their targets faster, but the effect also depends on the sliding lengths as well as the sliding rate. For short sliding lengths, pioneer TFs work much better than nonpioneer TFs. Increasing the sliding length modifies the dynamics, allowing nonpioneer TFs to find some targets faster. It was argued that this is the result of different transition rates for the dissociation from DNA and sliding along DNA for two types of transcription factors. Pioneer TFs prefer to be found

https://doi.org/10.1021/acs.jpclett.3c01704
J. Phys. Chem. Lett. 2023, 14, 7073−7082

in the nucleosome-covered region, where they also slide fast. The situation is the opposite for nonpioneer TFs that prefer to be found on free linker DNA. These differences explain the observed trends in the protein target search dynamics. It was also argued that in real systems the sliding lengths are most probably short, and it seems that pioneer TFs might be tuned by nature to take advantage of this. In addition, we found that nucleosome breathing has a much stronger effect on the protein target search for both types of TFs, and it is explained by the fact that the sliding is slower than the breathing.

Although the presented theoretical approach provides a reasonable microscopic picture of how nucleosome sliding might influence the search for target sites by different classes of TFs, it is important to discuss its limitations. Our theoretical model is based on several approximations. First, it was assumed that nucleosome sliding is a two-state process. However, in reality, it is a multistate process in which the nucleosome slides via many conformations that differ by only a single protein−DNA bond. This sequential mode of sliding might affect the overall search dynamics. Second, nucleosome dynamics (both sliding and breathing) are governed by a very complex free-energy landscape[29,65] that is not taken into account in our model. Indeed, all of our transition rates are assumed to be constant, while a more realistic free-energy landscape implies that they might be state- and position-dependent. Third, the effect of the DNA sequence has been neglected in our theoretical approach. However, despite these limitations, the important outcome of this study is the ability to explain complex biological phenomena using relatively simple physical-chemical ideas. In addition, there are specific quantitative predictions that might be tested by using advanced experimental and theoretical techniques.

■ ASSOCIATED CONTENT

Supporting Information

The Supporting Information is available free of charge at https://pubs.acs.org/doi/10.1021/acs.jpclett.3c01704.

Details of analytical calculations for the mean search times in the presence and absence of nucleosome sliding dynamics and in the presence of nucleosome breathing dynamics (PDF)

■ AUTHOR INFORMATION

Corresponding Author

Anatoly B. Kolomeisky − *Center for Theoretical Biological Physics, Rice University, Houston, Texas 77005, United States; Department of Chemistry and Department of Chemical and Biomolecular Engineering, Rice University, Houston, Texas 77005, United States;* orcid.org/0000-0001-5677-6690; Email: tolya@rice.edu

Author

Anupam Mondal − *Center for Theoretical Biological Physics, Rice University, Houston, Texas 77005, United States; Department of Chemistry, Rice University, Houston, Texas 77005, United States;* orcid.org/0000-0002-8436-5618

Complete contact information is available at: https://pubs.acs.org/10.1021/acs.jpclett.3c01704

Notes

The authors declare no competing financial interest.

■ ACKNOWLEDGMENTS

The work was supported by the Welch Foundation (C-1559), by the NSF (CHE-1953453 and CHE-2246878), and by the Center for Theoretical Biological Physics sponsored by the NSF (PHY-2019745).

■ REFERENCES

(1) Phillips, R.; Kondev, J.; Theriot, J.; Garcia, H. G.; Orme, N. *Physical biology of the cell*; Garland Science: New York, 2012.

(2) Lodish, H.; Berk, A.; Kaiser, C. A.; Krieger, M.; Scott, M. P.; Bretscher, A.; Ploegh, H.; Matsudaira, P. *Molecular cell biology*; Macmillan: New York, 2008.

(3) Iwahara, J.; Kolomeisky, A. B. Discrete-state stochastic kinetic models for target DNA search by proteins: theory and experimental applications. *Biophys Chem.* **2021**, *269*, 106521.

(4) Shvets, A. A.; Kochugaeva, M. P.; Kolomeisky, A. B. Mechanisms of protein search for targets on DNA: theoretical insights. *Molecules* **2018**, *23*, 2106.

(5) Onufriev, A. V.; Schiessel, H. The nucleosome: from structure to function through physics. *Curr. Opin Struct Biol.* **2019**, *56*, 119−130.

(6) Luger, K.; Mader, A. W.; Richmond, R. K.; Sargent, D. F.; Richmond, T. J. Crystal structure of the nucleosome core particle at 2.8 Å resolution. *Nature* **1997**, *389*, 251−260.

(7) Richmond, T. J.; Davey, C. A. The structure of DNA in the nucleosome core. *Nature* **2003**, *423*, 145−150.

(8) Harbison, C. T.; et al. Transcriptional regulatory code of a eukaryotic genome. *Nature* **2004**, *431*, 99−104.

(9) Wray, G. A.; Hahn, M. W.; Abouheif, E.; Balhoff, J. P.; Pizer, M.; Rockman, M. V.; Romano, L. A.; Wray, G. A. The evolution of transcriptional regulation in eukaryotes. *Mol. Biol. Evol.* **2003**, *20*, 1377−1419.

(10) Liu, X.; Lee, C. K.; Granek, J. A.; Clarke, N. D.; Lieb, J. D. Whole-genome comparison of Leu3 binding in vitro and in vivo reveals the importance of nucleosome occupancy in target site selection. *Genome Res.* **2006**, *16*, 1517−1528.

(11) Pique-Regi, R.; Degner, J. F.; Pai, A. A.; Gaffney, D. J.; Gilad, Y.; Pritchard, J. K. Accurate inference of transcription factor binding from DNA sequence and chromatin accessibility data. *Genome Res.* **2011**, *21*, 447−455.

(12) Brennan, L. D.; Forties, R. A.; Patel, S. S.; Wang, M. D. DNA looping mediates nucleosome transfer. *Nat. Commun.* **2016**, *7*, 13337.

(13) Miyagi, A.; Ando, T.; Lyubchenko, Y. L. Dynamics of nucleosomes assessed with time-lapse high-speed atomic force microscopy. *Biochemistry* **2011**, *50*, 7901−7908.

(14) Bilokapic, S.; Strauss, M.; Halic, M. Histone octamer rearranges to adapt to DNA unwrapping. *Nat. Struct Mol. Biol.* **2018**, *25*, 101−108.

(15) Polach, K. J.; Widom, J. Mechanism of protein access to specific DNA sequences in chromatin: a dynamic equilibrium model for gene regulation. *J. Mol. Biol.* **1995**, *254*, 130−149.

(16) Kim, J.; Lee, J.; Lee, T. H. Lysine acetylation facilitates spontaneous DNA dynamics in the nucleosome. *J. Phys. Chem. B* **2015**, *119*, 15001−15005.

(17) Li, G.; Levitus, M.; Bustamante, C.; Widom, J. Rapid spontaneous accessibility of nucleosomal DNA. *Nat. Struct Mol. Biol.* **2005**, *12*, 46−53.

(18) Li, G.; Widom, J. Nucleosomes facilitate their own invasion. *Nat. Struct Mol. Biol.* **2004**, *11*, 763−769.

(19) Tims, H. S.; Gurunathan, K.; Levitus, M.; Widom, J. Dynamics of nucleosome invasion by DNA binding proteins. *J. Mol. Biol.* **2011**, *411*, 430−448.

(20) Winogradoff, D.; Aksimentiev, A. Molecular mechanism of spontaneous nucleosome unraveling. *J. Mol. Biol.* **2019**, *431*, 323−335.

(21) Armeev, G. A.; Kniazeva, A. S.; Komarova, G. A.; Kirpichnikov, M. P.; Shaytan, A. K. Histone dynamics mediate DNA unwrapping and sliding in nucleosomes. *Nat. Commun.* **2021**, *12*, 2387.

(22) Mondal, A.; Mishra, S. K.; Bhattacherjee, A. Kinetic origin of nucleosome invasion by pioneer transcription factors. *Biophys. J.* **2021**, *120*, 5219−5230.
(23) Mondal, A.; Mishra, S. K.; Bhattacherjee, A. Nucleosome breathing facilitates cooperative binding of pluripotency factors Sox2 and Oct4 to DNA. *Biophys. J.* **2022**, *121*, 4526−4542.
(24) Mondal, A.; Felipe, C.; Kolomeisky, A. B. Nucleosome breathing facilitates the search for hidden DNA sites by pioneer transcription factors. *J. Phys. Chem. Lett.* **2023**, *14*, 4096−4103.
(25) Hodges, C.; Bintu, L.; Lubkowska, L.; Kashlev, M.; Bustamante, C. Nucleosomal fluctuations govern the transcription dynamics of RNA polymerase II. *Science* **2009**, *325*, 626−628.
(26) Bintu, L.; Kopaczynska, M.; Hodges, C.; Lubkowska, L.; Kashlev, M.; Bustamante, C. The elongation rate of RNA polymerase determines the fate of transcribed nucleosomes. *Nat. Struct Mol. Biol.* **2011**, *18*, 1394−1399.
(27) Farr, S. E.; Woods, E. J.; Joseph, J. A.; Garaizar, A.; Collepardo-Guevara, R. Nucleosome plasticity is a critical element of chromatin liquid-liquid phase separation and multivalent nucleosome interactions. *Nat. Commun.* **2021**, *12*, 2883.
(28) Brandani, G. B.; Niina, T.; Tan, C.; Takada, S. DNA sliding in nucleosomes via twist defect propagation revealed by molecular simulations. *Nucleic Acids Res.* **2018**, *46*, 2788−2801.
(29) Lequieu, J.; Schwartz, D. C.; de Pablo, J. J. In silico evidence for sequence-dependent nucleosome sliding. *Proc. Natl. Acad. Sci. U. S. A.* **2017**, *114*, E9197−E9205.
(30) Bai, L.; Morozov, A. V. Gene regulation by nucleosome positioning. *Trends Genet* **2010**, *26*, 476−483.
(31) Nocetti, N.; Whitehouse, I. Nucleosome repositioning underlies dynamic gene expression. *Genes Dev.* **2016**, *30*, 660−672.
(32) Mueller-Planitz, F.; Klinker, H.; Becker, P. B. Nucleosome sliding mechanisms: new twists in a looped history. *Nat. Struct Mol. Biol.* **2013**, *20*, 1026−1032.
(33) Struhl, K.; Segal, E. Determinants of nucleosome positioning. *Nat. Struct Mol. Biol.* **2013**, *20*, 267−273.
(34) Chereji, R. V.; Clark, D. J. Major determinants of nucleosome positioning. *Biophys. J.* **2018**, *114*, 2279−2289.
(35) Niina, T.; Brandani, G. B.; Tan, C.; Takada, S. Sequence-dependent nucleosome sliding in rotation-coupled and uncoupled modes revealed by molecular simulations. *PLoS Comput. Biol.* **2017**, *13*, No. e1005880.
(36) Hamiche, A.; Kang, J. G.; Dennis, C.; Xiao, H.; Wu, C. Histone tails modulate nucleosome mobility and regulate ATP-dependent nucleosome sliding by NURF. *Proc. Natl. Acad. Sci. U. S. A.* **2001**, *98*, 14316−14321.
(37) Flaus, A.; Rencurel, C.; Ferreira, H.; Wiechens, N.; Owen-Hughes, T. Sin mutations alter inherent nucleosome mobility. *EMBO J.* **2004**, *23*, 343−353.
(38) Morioka, S.; Sato, S.; Horikoshi, N.; Kujirai, T.; Tomita, T.; Baba, Y.; Kakuta, T.; Ogoshi, T.; Puppulin, L.; Sumino, A.; Umeda, K.; Kodera, N.; Kurumizaka, H.; Shibata, M. High-speed atomic force microscopy reveals spontaneous nucleosome sliding of H2A.Z at the subsecond time scale. *Nano Lett.* **2023**, *23*, 1696−1704.
(39) Rudnizky, S.; Khamis, H.; Malik, O.; Melamed, P.; Kaplan, A. The base pair-scale diffusion of nucleosomes modulates binding of transcription factors. *Proc. Natl. Acad. Sci. U. S. A.* **2019**, *116*, 12161−12166.
(40) Mishra, S. K.; Bhattacherjee, A. How do nucleosome dynamics regulate protein search on DNA? *J. Phys. Chem. B* **2023**, *127*, 5702−5717.
(41) Tang, X.; Li, T.; Liu, S.; Wisniewski, J.; Zheng, Q.; Rong, Y.; Lavis, L. D.; Wu, C. Kinetic principles underlying pioneer function of GAGA transcription factor in live cells. *Nat. Struct Mol. Biol.* **2022**, *29*, 665−676.
(42) Iwafuchi-Doi, M.; Zaret, K. S. Cell fate control by pioneer transcription factors. *Development* **2016**, *143*, 1833−1837.
(43) Iwafuchi-Doi, M.; Zaret, K. S. Pioneer transcription factors in cell reprogramming. *Genes Dev.* **2014**, *28*, 2679−2692.
(44) Zaret, K. S.; Mango, S. E. Pioneer transcription factors, chromatin dynamics, and cell fate control. *Curr. Opin Genet Dev* **2016**, *37*, 76−81.
(45) Zaret, K. S.; Carroll, J. S. Pioneer transcription factors: establishing competence for gene expression. *Genes Dev.* **2011**, *25*, 2227−2241.
(46) Slattery, M.; Zhou, T.; Yang, L.; Dantas Machado, A. C.; Gordan, R.; Rohs, R. Absence of a simple code: how transcription factors read the genome. *Trends Biochem. Sci.* **2014**, *39*, 381−399.
(47) Iwafuchi-Doi, M.; Donahue, G.; Kakumanu, A.; Watts, J. A.; Mahony, S.; Pugh, B. F.; Lee, D.; Kaestner, K. H.; Zaret, K. S. The pioneer transcription factor FoxA maintains an accessible nucleosome configuration at enhancers for tissue-specific gene activation. *Mol. Cell* **2016**, *62*, 79−91.
(48) Zaret, K. S. Pioneer transcription factors initiating gene network changes. *Annu. Rev. Genet* **2020**, *54*, 367−385.
(49) Cirillo, L. A.; McPherson, C. E.; Bossard, P.; Stevens, K.; Cherian, S.; Shim, E. Y.; Clark, K. L.; Burley, S. K.; Zaret, K. S. Binding of the winged-helix transcription factor HNF3 to a linker histone site on the nucleosome. *EMBO J.* **1998**, *17*, 244−254.
(50) Cirillo, L. A.; Lin, F. R.; Cuesta, I.; Friedman, D.; Jarnik, M.; Zaret, K. S. Opening of compacted chromatin by early developmental transcription factors HNF3 (FoxA) and GATA-4. *Mol. Cell* **2002**, *9*, 279−289.
(51) Soufi, A.; Garcia, M. F.; Jaroszewicz, A.; Osman, N.; Pellegrini, M.; Zaret, K. S. Pioneer transcription factors target partial DNA motifs on nucleosomes to initiate reprogramming. *Cell* **2015**, *161*, 555−568.
(52) Felipe, C.; Shin, J.; Kolomeisky, A. B. How pioneer transcription factors search for target sites on nucleosomal DNA. *J. Phys. Chem. B* **2022**, *126*, 4061−4068.
(53) Felipe, C.; Shin, J.; Loginova, Y.; Kolomeisky, A. B. The effect of obstacles in multi-site protein target search with DNA looping. *J. Chem. Phys.* **2020**, *152*, 025101.
(54) Donovan, B. T.; Chen, H.; Jipa, C.; Bai, L.; Poirier, M. G. Dissociation rate compensation mechanism for budding yeast pioneer transcription factors. *Elife* **2019**, *8*, e43008.
(55) Luo, Y.; North, J. A.; Rose, S. D.; Poirier, M. G. Nucleosomes accelerate transcription factor dissociation. *Nucleic Acids Res.* **2014**, *42*, 3017−3027.
(56) Luo, Y.; North, J. A.; Poirier, M. G. Single molecule fluorescence methodologies for investigating transcription factor binding kinetics to nucleosomes and DNA. *Methods* **2014**, *70*, 108−118.
(57) Donovan, B. T.; Chen, H.; Eek, P.; Meng, Z.; Jipa, C.; Tan, S.; Bai, L.; Poirier, M. G. Basic helix-loop-helix pioneer factors interact with the histone octamer to invade nucleosomes and generate nucleosome-depleted regions. *Mol. Cell* **2023**, *83*, 1251−1263.
(58) Veksler, A.; Kolomeisky, A. B. Speed-selectivity paradox in the protein search for targets on DNA: is it real or not? *J. Phys. Chem. B* **2013**, *117*, 12695−12701.
(59) Mondal, A.; Bhattacherjee, A. Understanding the role of DNA topology in target search dynamics of proteins. *J. Phys. Chem. B* **2017**, *121*, 9372−9381.
(60) Singh, A. K.; Mueller-Planitz, F. Nucleosome positioning and spacing: from mechanism to function. *J. Mol. Biol.* **2021**, *433*, 166847.
(61) Valouev, A.; Johnson, S. M.; Boyd, S. D.; Smith, C. L.; Fire, A. Z.; Sidow, A. Determinants of nucleosome organization in primary human cells. *Nature* **2011**, *474*, 516−520.
(62) Bowman, G. D. Mechanisms of ATP-dependent nucleosome sliding. *Curr. Opin Struct Biol.* **2010**, *20*, 73−81.
(63) Becker, P. B. Nucleosome sliding: facts and fiction. *EMBO J.* **2002**, *21*, 4749−4753.
(64) Nizovtseva, E. V.; Clauvelin, N.; Todolli, S.; Polikanov, Y. S.; Kulaeva, O. I.; Wengrzynek, S.; Olson, W. K.; Studitsky, V. M. Nucleosome-free DNA regions differentially affect distant communication in chromatin. *Nucleic Acids Res.* **2017**, *45*, 3059−3067.

https://doi.org/10.1021/acs.jpclett.3c01704
J. Phys. Chem. Lett. 2023, 14, 7073−7082

(65) Zhang, B.; Zheng, W.; Papoian, G. A.; Wolynes, P. G. Exploring the free energy landscape of nucleosomes. *J. Am. Chem. Soc.* **2016**, *138*, 8126−8133.

https://doi.org/10.1021/acs.jpclett.3c01704
J. Phys. Chem. Lett. 2023, 14, 7073−7082